A 10 GHz Active Annular Ring Antenna *

Joseph A. Hagerty and Zoya Popović

Joseph.Hagerty@Colorado.EDU
Department of Electrical and Computer Engineering,
University of Colorado
Boulder, CO 80309-0425 USA

Abstract

An X-band oscillating element can be achieved in compact form with high-efficiency operation and high isotropic conversion gain. An annular ring is used here both as the radiating element and microstrip feedback circuit for the amplifier. A maximum dc-rf conversion efficiency for co-polarized radiated power is 55% at 10 GHz with maximum effective radiated power of 23.6 dBm and total radiated power of 15.5 dBm. The active ring is a good candidate for high aperture efficiency spatial power combining arrays and compact low-cost wireless sensors.

1 Introduction

Free-space power combining of distributed oscillating elements presents a high-efficiency solution to microwave dc-rf conversion. By distributing sources in an array, transmission lines, combiners, and associated losses can be eliminated. Furthermore, the circuit size of the individual oscillating elements can be greatly reduced by incorporating the antenna element directly as a resonator and feedback circuit. Early designs have combined the radiating element as a load with a stand-alone oscillator and separate feedback loop. More recent designs have used rectangular patches as a radiator in the feedback path [1]. FETs were also directly integrated into the radiating element using modified antenna geometries for direct matching [2].

Here we investigate the additional advantages of using a compact single- layer high gain switched mode integrated oscillating antenna. The performance of the unit cell is assessed as an element for a high- efficiency power combining array. A microstrip annular ring has been chosen to improve the radiation characteristics and reduce microstrip circuitry over conventional designs. The entire circuit is conveniently enclosed inside the ring allowing for strait-forward, compact array design. High-efficiency is afforded by switched mode transistor operation, high antenna gain, and high array packing density.

High-efficiency, switched mode operation is achieved with class-E operation of the amplifier stage: At the output, wave shaping is performed at the fundamental and second harmonic, forcing the transistor to operate as a switch, while the current delivered to the load is sinusoidal [4]. In this paper, the techniques used for class-E matching and feedback for oscillation are modified for integration with a 2-port antenna. The antenna is designed as a 2-port structure with tunable coupling so that an additional coupler is not needed.

2 Antenna design

Several performance considerations have been put to the geometrical design of the annular ring as a radiator and selective feedback structure. The geometry of the annular ring was designed

*This work was supported by an ARO MURI in Quasi-Optical Power Combining, grant DAAOH-98-0001 and an NSF special program under Grant NCR 9725778.

0-7803-7330-8/02 $17.00 © 2002 IEEE

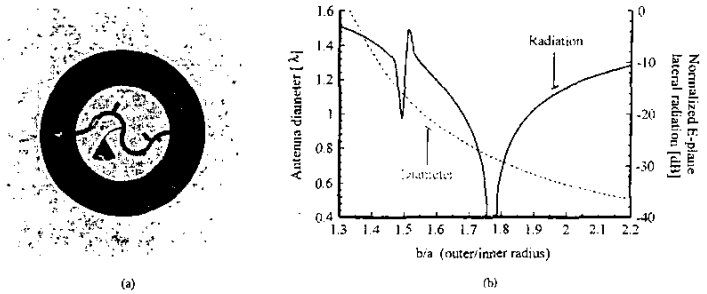

Figure 1: (a) Photograph of the microstrip annular ring with MESFET and high-efficiency circuit. The input impedance of the antenna feed is matched to the FET for the high efficiency operation. The input matching circuit to the left of the device controls the degree of feedback. The outer diameter of the ring is $0.72\,\lambda_0$ at 10 GHz. (b) Lateral radiated power normalized to broadside and antenna diameter as a function of b/a ratio for a 10 GHz ring on a TMM10i substrate with ϵ_r=9.8.

for radiative and selective feedback properties simultaneously. The ring predominately supports circumferential and radial transverse magnetic field variations, denoted n and m. For the TM_{n1} modes, the field varies only along the circumference and subsequent resonances are narrow band compared to higher order modes. Theoretical field analysis was performed using Zeland *IESD* MoM solver for current distributions on the patch and radiation patterns. Additional radiation behavior and modal analysis were studied using expressions derived from the cavity model of the ring [5]. Here, the TM_{12} mode is used for several reasons. Despite its considerably higher operating frequency compared to the fundamental TM_{11} mode, the TM_{12} mode is used for its wider bandwidth. In our case, the wider bandwidth allows for higher tolerances in design and fabrication errors while maintaining a stable oscillation. Furthermore, the ratio of the outer to inner radii, b/a, can be designed to improve radiation characteristics such as side-lobe level and lateral radiation as shown in Fig. 1(b). In effect, radiation from opposing sides of the ring can be designed to cancel lateral radiation in the E-plane, boosting the antenna gain and decreasing the coupling between arrayed elements [6].

Since several TM_{n1} modes occur at lower frequencies than the TM_{12} mode, care must be taken to ensure that none of these modes meet an oscillation condition or overlap with the desired TM_{12} mode. The choice of b/a ratio can also be chosen to design unwanted modes out of the desired operation. This is shown in Fig. 2(a) where the modes are charted as a function of b/a ratio relative to a 10 GHz resonant TM_{12} mode at that ratio. Fig. 3(b) demonstrates the measured and simulated return loss and mode occurrence of the ring in a 50 Ω system.

3 Integrated Class-E Annular Ring

The annular ring and class-E circuit with matching sections are designed separately and then analyzed as a complete circuit. Considering ports 1 and 2 of the ring as shown in Fig. 3(a), the input impedance, Z_{11}, of the antenna must be transformed to the class-E match, while S_{21} quantifies the feedback coupling factor. The magnitude of feedback coupling can be determined by the load

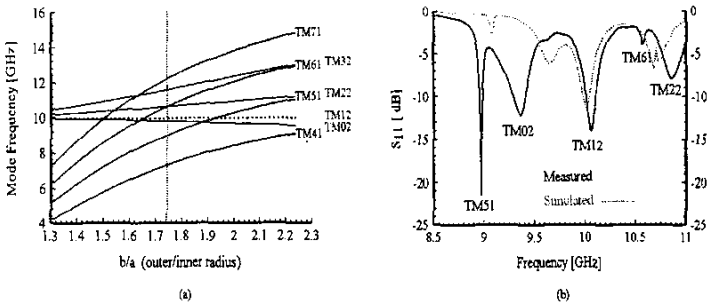

Figure 2: (a) Simulated resonant frequency of adjacent modes to the TM_{12} mode as a function of b/a ratio. For each geometry, the antenna is scaled so that the TM_{12} mode is resonant at 10 GHz. The vertical line represents the particular b/a ratio chosen here. (b) Measured return loss of the passive microstrip annular ring.

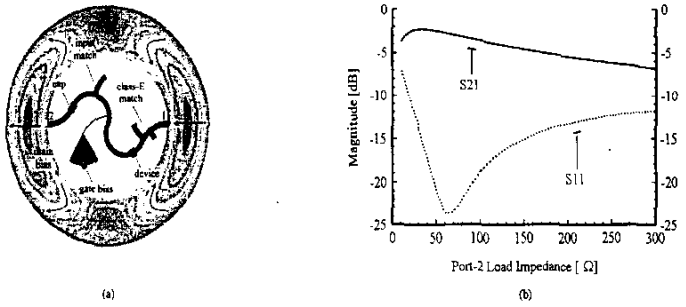

Figure 3: (a) Layout of the integrated ring with simulated average current amplitude distribution. Arrows indicate current density field lines. (b) Simulated coupling factor and consequent change in return loss as a function of load presented to port 2 of (a).

presented to port 2 of the antenna. The amount of coupling and return loss at port 1 as a function of the load at port 2 is shown in Fig. 3(b). In the present case, a load of 280 Ω was chosen for -6.4 dB (23%) feedback. A line length is added to the input matching circuit to complete the $2\pi n$ closed loop phase while matching the transistor input to 280 Ω. As expected from the simulated current distribution on the ring, the phase of S_{21} across the antenna is calculated to be just under π. while the transistor S_{21} phase is a little less than $\pi/2$. Therefore, the microstrip circuitry must add over $\pi/2$ in phase. forcing it to meander inside the ring. Full-wave field analysis combined with measurements on a single-port passive ring are then used to calculate the 2-port antenna parameters.

4 Measurements

All measurements on the active ring were performed in a 4 m anechoic chamber. Broadside radiated power, oscillation frequency, and drain current were recorded over 644 bias points (from V_{gs} =

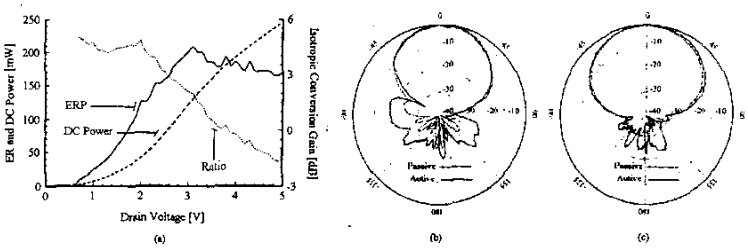

Figure 4: (a) EIR and DC power as a function of drain voltage for Vgs=-1.3 V. (b) Active and passive E-plane co-polarized patterns. (c) Active and passive H-plane co-polarized patterns.

$-0.6\,V$ and $V_{ds} = 0.6\,V$ to $V_{gs} = -2\,V$ and $V_{ds} = 5\,V$) using a computerized bias sweep of the gate and drain. The total radiated power and efficiency are calculated relative to a passive ring. The frequency of oscillation across the entire bias sweep varies by 1.5% of the design frequency. The measured ERP and DC power consumption for $V_{gs} = -1.3\,V$ are shown in Fig. 4(a) as a function of drain bias.

Measured radiation patterns at various bias points do not vary considerably as expected from the antenna bandwidth shown in Fig. 2(b). Figs. 4(b) and 4(c) show a comparison between the measured passive and active E and H-planes. The cross-polarized power at boresight is -28 dB. The laterally radiated power at 90° agrees well with the predicted values of Fig. 1(b) for a value of $b/a = 1.75$. The bias lines contribute to increased back-side radiation for the active ring. The isotropic conversion gain is a measure of the active antenna's gain and dc-rf efficiency and is shown in Fig. 4(a) in dotted line along with the ERP.

References

[1] R.D. Martinez and R.C. Compton, "High-efficiency FET/microstrip-patch oscillators," *IEEE Antennas and Propagation Magazine*, vol. 36, no. 1, pp. 16–19, Feb. 1994.

[2] C. Ho and K. Chang, "New FET active slotline ring antenna," *Electron. Lett.*, vol. 29, pp. 521–522, Mar. 1993.

[3] M.M. Kaleja and E.M. Biebl et al., "Low-cost automobile crash-sensor using a 61 GHz active integrated SIMMWIC antenna," *IEEE MTT-S Int. Microwave Symp. Dig.*, vol. 3, pp. 1969–1972, 2000.

[4] E.W. Bryerton, W.A. Shiroma, and Z. Popović, "A 5-GHz high efficiency class-e oscillator," *IEEE Microwave and Guided Wave Lett.*, vol. 6, no. 12, pp. 441–443, Dec. 1996.

[5] A. Bhattacharyya and R. Garg, "Analysis of annular ring microstrip antenna using cavity model," *Archiv für Elektronik und Übertragungstechnik*, vol. 39, pp. 185–189, 1985.

[6] M.A. Khayat, J.T. Williams, D.R. Jackson, and S.A. Long, "Mutual coupling between reduced surface-wave microstrip antennas," *IEEE Trans. Ant. and Prop.*, vol. 48, no. 10, pp. 1581–1593, Oct. 2000.